Journal of the European Ceramic Society 22 (2002) 1357–1365

www.elsevier.com/locate/jeurceramsoc

Thermal shock properties of β-sialon ceramics

Pernilla Pettersson, Zhijian Shen, Mats Johnsson*, Mats Nygren

Department of Inorganic Chemistry, Stockholm University, S-106 91 Stockholm, Sweden

Received 8 June 2001; accepted 2 August 2001

Abstract

An indentation–quench method based on Vickers cracks for measuring thermal-shock properties has been applied to β-sialon materials. The thermal-shock properties have been correlated with the morphology of the β-sialon grains, the z value in the β-sialon solid solution $Si_{6-z}Al_zO_zN_{8-z}$ and the amount of residual intergranular glass phase. z Values in the range 0.6–3.0 were tested, and the amount of residual yttrium-containing glass phase was varied between 0 and 20 vol.%. The best thermal-shock resistance was found at low z values, and was further improved by adding an intergranular glass phase. The poorest resistance to thermal shock was found for the highest z value where the presence of glass had no measurable influence. One composition ($z=1.5$, 10 vol.% glass) was selected for studying the influence of the microstructure on the thermal-shock properties. The microstructure was varied by applying different sintering conditions. An improvement of the thermal-shock properties and the fracture toughness was found in samples containing elongated β-sialon grains formed in situ. In general, in-situ reinforced β-sialon materials with low z values and containing an intergranular glass phase exhibited the best thermal-shock resistance and improved fracture toughness ($K_{1c}>4$ MPa $m^{\frac{1}{2}}$).

Keywords: Indentation; Mechanical properties; Microstructure-final; Sialons; Thermal shock resistance

1. Introduction

β-sialon, represented by the formula $Si_{6-z}Al_zO_zN_{8-z}$ ($0\leqslant z<4.2$), is a solid-solution phase with a structure similar to hexagonal β-Si_3N_4. Ceramics based on the β-sialon phase are a series of well-commercialised materials prepared in large volumes for various engineering applications, preferably at temperatures below 1000 °C. Without additives, though, monophasic β-sialon ceramics are difficult to compact pressure-less due to the lack of a liquid phase, and processes such as hot pressing (HP), hot isostatic pressing (HIP), and spark plasma sintering (SPS) have been applied to prepare fully compacted bodies. Even very small additions of sintering aids improve the densification kinetics dramatically, implying that components of very complex shape, made of β-sialon based ceramics, can be compacted to theoretical density by pressure-less sintering techniques.

The SPS technique provided the best possibilities to control the microstructure. By altering the sintering temperature, pressure and the sintering time, the microstructure could be controlled so that the morphology of the formed β-sialon grains was varied between equiaxed and well-developed elongated shape.

As β-sialon-based ceramics are used for applications such as load-bearing components, their mechanical properties, e.g. flexure strength, fracture toughness, hardness, and high-temperature creep resistance, have been extensively studied.[1] However, comparatively little attention has been paid to their thermal-shock properties. Up to now, there have been no systematic studies of the correlation between thermal-shock properties and structural and chemical compositional parameters of β-sialon materials, e.g. of the formed β-sialon grains, and the amount of residual intergranular glass present. Neither are there any reports on correlation between the microstructure and the thermal-shock properties. Such correlations ought to be of great importance in applications where resistance to thermal cycling is a prerequisite, i.e. for cutting-tool inserts and molten-metal handling pipes.

Various methods have been developed over the years to measure the thermal-shock properties of various materials. Most of these methods are based on test bars,

* Corresponding author. Tel.: +46-8-674-7067; fax: +46-8-152187.
E-mail address: matsj@inorg.su.se (M. Johnsson).

0955-2219/02/$ - see front matter
PII: S0955-2219(01)00429-0

of specified dimensions and geometries, which are heated to thermal equilibrium in a furnace, then quenched in a water bath, and subsequently subjected to three- or four-point bending-strength tests.[2–5] The manufacturing of test bars with well-defined shape and surface finish is complicated. In that type of investigation, each test bar can only be used once, implying that separate bars are required for each temperature to be tested, and in order to improve statistics several bars are normally tested at each temperature. Using these methods is thus both time-consuming and costly, which complicates the evaluation of thermal-shock properties.

Andersson and Rowcliffe[6] have developed a method to determine such properties based on making small initial Vickers cracks on a polished plate of defined thickness of the material to be tested. The indented plate is heated in a vertical tube furnace and subsequently quenched in a water bath, and the crack growth is measured and correlated with the temperature difference between the furnace and the water bath. The growth is measured as an average percentage of the original crack length. The method allows the same sample to be used throughout a test series of different quenching temperatures, and the statistics are improved by measuring the crack growth for several indentations made on the same sample. Pettersson et al.[7] have studied the influence of different experimental parameters when using this indentation-quench method. The method provides us with an efficient way of obtaining comparable thermal-shock data for materials of similar compositions, and we have used it to perform systematic studies of sialon-based ceramics.

In this article, we report the thermal-shock properties of β-sialon-based materials prepared with and without additions of sintering aids i.e. β-sialons with different z values where also the amount of intergranular glass phase is varied. The sintering conditions were varied for one selected composition, which yielded different types of microstructures. The relation between these microstructures and the thermal-shock properties is discussed.

2. Experimental

2.1. Sample preparation

Three series of β-sialon samples were prepared in the present work. Samples of series A were designed to give pure β-sialon ceramics with z values of 0.6, 1.0, 1.5, 2.0 and 3.0. In the B series, 5, 10 and 20 vol.% of a secondary intergranular glass phase was added to the A series compositions, see Table 1. This added glass phase had the nominal overall composition $Y_{1.75}Si_{2.625}Al_{1.0}O_{7.5}N_{1.25}$ (28Y; 56Si; 16Al; 80O; 20N in equivalent%[1]). In the C series, the sintering conditions of the β-sialon with $z = 1.5$ and 10 vol.% glass were varied, yielding different microstructures.

Table 1
Overall compositions of the starting materials (in wt.%)

Sample	Nominal z value	GP vol. % [a]	Y_2O_3	Si_3N_4	AlN	Al_2O_3	SiO_2
A series							
A1	0.6	–	–	90.41	5.29	4.33	–
A2	1.0	–	–	83.60	7.09	9.33	–
A3	1.5	–	–	75.12	9.33	15.56	–
A4	2.0	–	–	66.67	11.57	21.87	–
A5	3.0	–	–	49.84	16.03	34.14	–
B series							
B1	0.6	5	2.75	87.14	3.73	6.37	–
B2	0.6	10	5.48	83.94	2.19	8.38	–
B3	0.6	20	10.84	73.33	4.14	6.19	5.49
B4	1.0	10	5.50	77.86	3.78	12.85	–
B5[b]	1.5	10	5.53	70.28	5.76	18.41	–
B6	2.0	10	5.56	62.74	7.73	23.95	–
B7	3.0	5	2.83	48.80	13.82	34.55	–
B8	3.0	10	5.63	47.77	11.64	34.95	–
B9	3.0	20	11.11	45.75	7.37	35.75	–

[a] The designed amount of a secondary intergranular amorphous glass phase (GP) in volume percent.
[b] This composition was used also for preparation of series C.

Specimens were prepared from commercial Si_3N_4 (UBE, SN-E10), AlN (H.C. Starck-Berlin, grade A), Y_2O_3 (99.9%, Johnson Matthey Chemicals Ltd.), Al_2O_3 (Alcoa, A16SG) and SiO_2 (99.9%, <325 mesh, Johnson Matthey Chemicals Ltd.), and corrections were made for the small amounts of oxygen present in the Si_3N_4 and AlN raw materials. The starting-material mixtures were milled in water-free propanol for 24 h in a plastic jar, using sialon milling media. The dried powder mixtures were sintered by hot pressing (Thermal Technology Inc.) for 90 min at a temperature of 1750 °C and a pressure of 30 MPa, in order to ensure full density. The starting powder mixture was loaded in a cylindrical carbon die with an inner diameter of 12 mm. The samples A2 and A3, see below, had to be hot-isostatically pressed for 60 min at a temperature of 1820 °C and a pressure of 200 MPa in order to become fully dense. Sample A1 could not be fully densified by the hot-isostatic pressing technique but, using the spark plasma sintering (SPS) technique, fully dense samples were obtained at 1700 °C and a pressure of 50 MPa with a holding time of 3 min. The obtained densities matched those obtained by Ekström et al.[8] and the samples were thus considered fully dense.

The samples in series C were prepared by the SPS technique at temperatures in the range 1500–1600 °C, at a pressure of 50 MPa and with holding times between 0 and 15 min. By adjustment of the processing conditions, different microstructures were obtained, i.e. samples consisting of sub-micro equiaxed grains, ultra-fine elongated grains and well-developed elongated grains. The thermal-shock behaviour of this series of samples was used to evaluate the relation between microstructure

and thermal-shock resistance. The preparation conditions, phase composition, density, hardness and fracture toughness of the prepared samples are given in Table 2.

The SPS processing was carried out in vacuum in a spark-plasma sintering apparatus, Dr. Sinter 2050 (Sumitomo Coal Mining Co. Ltd., Japan). The powder precursors were loaded in a cylindrical carbon die with an inner diameter of 12 mm in the same way as for the hot-pressing experiments. From 600 °C and up, the temperature was monitored by an optical pyrometer focused on the surface of the die, and a heating rate of 100 °C/min was applied.

2.2. Characterisation techniques

The densities of the sintered specimens were measured according to Archimedes' principle. Before the studies of mechanical and microstructural characteristics, the specimens were carefully polished by standard diamond polishing techniques. The hardness (H_{v10}) and indentation fracture toughness (K_{1C}) at room temperature were obtained with a Vickers diamond indenter with a 98 N load, and the fracture toughness was evaluated according to the method of Anstis et al.[9], assuming a value of 300 GPa for Young's modulus. Five indentations were made in each sample, and the average is given. The sample microstructures were investigated in a scanning electron microscope (SEM, Jeol 880) equipped with an energy-dispersive spectrometer (EDS, LINK *ISIS*). To obtain the best contrast between different phases, the micrographs were recorded in back-scattered electron mode (BSE) at an acceleration voltage of 20 kV. The amounts of intergranular glass phase in series B were evaluated with an image-analysing package supplied with the LINK *ISIS* system. Images were collected at 10 kV acceleration voltage, and the contrast difference between the β-sialon grains and the yttrium-containing glass phase was used to estimate the phase content in

Table 2
The different SPS sintering conditions used to prepare the samples in series C and the resulting phase composition and β-sialon morphology

Sample	Sintering temperature (°C)	Dwelling time (min)	Phase composition	Morphology
C1	1500	15	β + 8%α	Sub-micro equiaxed
C2	1550	5	β + 8%α	Sub-micro equiaxed
C3	1550	15	β	Ultra-fine elongated
C4	1600	0.5	β	Ultra-fine elongated
C5	1600	15	β	Well developed elongated

Table 3
The measured z value and unit cell parameters for the β-sialon phase in the prepared samples and their densities, H_V and K_{1C} values

Sample	Unit cell dimension a-axis (Å)	Unit cell dimension c-axis (Å)	Measured z value	Measured vol. % glass	Measured density (g/cm^3)	H_V (GPa)	K_{1c} (MPa m$^{1/2}$)
A series							
A1	7.6178(3)	2.9187(2)	0.5		3.16	15.2	2.2
A2	7.6308(4)	2.9298(3)	0.9		3.07	16.0	2.6
A3	7.6462(2)	2.9425(1)	1.4		3.06	16.1	4.2
A4	7.6497(6)	2.9471(4)	1.6		3.13	16.6	2.5
A5	7.6791(6)	2.9719(5)	2.6		3.15	15.7	2.6
B series							
B1	7.6204(3)	2.9210(1)	0.6	6	3.20	17.9	4.2
B2	7.6205(3)	2.9201(2)	0.6	10	3.21	18.0	4.1
B3	7.6211(4)	2.9186(3)	0.5	26	3.26	15.8	5.3
B4	7.6324(5)	2.9302(5)	1.0	11	3.20	17.1	4.4
B5	7.6492(6)	2.9426(4)	1.5	14	3.19	17.4	3.8
B6	7.6616(4)	2.9542(3)	1.9	14	3.17	16.3	3.4
B7	7.6865(9)	2.9794(4)	2.8	5	3.10	15.1	2.5
B8	7.6849(9)	2.9783(6)	2.8	9	3.13	15.0	2.9
B9	7.6834(4)	2.9740(2)	2.7	18	3.16	14.9	2.9
C series							
C1	7.6527(9)	2.9454(9)	1.6		3.19	16.7	3.5
C2	7.6503(8)	2.9452(5)	1.6		3.20	17.2	3.7
C3	7.6483(7)	2.9421(4)	1.5		3.19	16.8	4.0
C4	7.6474(7)	2.9420(4)	1.4		3.18	16.7	4.0
C5	7.6460(4)	2.9411(3)	1.4		3.18	17.1	4.4

vol.%, which was assumed valid for the whole sample volume. The estimated minimum and maximum amounts of glass phase gave an error of 1%.

A focusing X-ray powder diffraction camera of Guinier-Hägg type with Cu$K_{\alpha 1}$ radiation ($\lambda = 1.5405981$ Å) was used to record the X-ray powder diffraction (XRD) patterns, and powdered silicon ($a = 5.430879$ Å at 25 °C) was added as internal standard. The computer programs SCANPI[10] and PIRUM[11] were used to evaluate the recorded films. The latter program was also used to determine and refine the unit cell parameters. The z value of the β-sialon phase was obtained from its unit cell dimensions, using the equations given by Ekström et al.[8], see Table 3.

Nominal z values and nominal glass contents are used in the discussion below, if not otherwise stated.

2.3. Thermal shock measurements

Experimental parameters of the indentation-quench method, such as sample thickness, crack length and water bath temperature, were selected according to the findings of Pettersson et al.[7] Cylindrical samples, with a diameter of 12 mm and a thickness of 3.86 0.42 mm, were ground to make the two flat surfaces parallel, and one of these was then carefully polished. Well-defined cracks were initiated with a Vickers indenter. Four indents were made on each sample, implying that sixteen cracks were initiated. In order to make the comparison of different samples easier, the original crack length was held constant around 100 μm. The indenting load was optimised to give cracks of the desired size for different materials (see Table 4). The crack length was measured in an optical microscope (Olympus PMG3). A vertical tubular furnace was heated to the starting temperature, 190 °C, the sample was hoisted into the furnace, thermally equilibrated for 20 min and then quenched in a thermostated 90 °C water bath. The heating and quenching procedure was then repeated at temperatures stepwise increased by 100 °C. The test pieces were heated in air, and only a slight oxidation was observed at the highest temperatures. The samples were only exposed to temperatures below 1100 °C, in order to avoid severe surface oxidation.[12] The crack growth was measured at each temperature, and the total percentage growth (Δc) was calculated. We have ranked the thermal-shock resistance of the studied materials by comparing the temperature difference inducing 10% growth of the initial cracks (ΔT_{10}). This value was found from a linear fit of all $\Delta T - \Delta c$ values measured for a sample.

Table 4
Sample thickness, indentation load and initial crack length for all samples used in measuring thermal-shock properties

Sample	Sample thickness (mm)	Indentation load (N)	Initial crack length (μm)
A1	4.04	35	91
A2	3.94	30	93
A3	4.04	35	100
A4	4.16	35	99
A5	3.74	40	103
B1	3.32	62	103
B2	4.16	60	98
B3	3.24	70	104
B4	4.13	60	99
B5	4.16	55	98
B6	4.15	40	88
B7	3.09	44	119
B8	3.23	40	112
B9	3.14	49	121
C1	4.17	35	87
C2	4.11	35	84
C3	4.17	40	84
C4	4.20	55	101
C5	4.22	55	101

3. Results and discussion

3.1. Microstructural evaluation

The SEM micrographs given in Figs. 1a–c show the fractured surfaces of series A β-sialons with z values of 0.6, 1.5 and 3.0, respectively, prepared without addition of sintering aid. The grain size of the β-sialon phase increases with increasing z value. The morphology of the formed β-sialon grains appears to be equiaxed; as no or very little intergranular glass phase was present. This is in accordance with the knowledge that a certain amount of liquid phase facilitate the formation of elongated β-sialon via a dissolution-precipitation mechanism.[13] Minor amounts of an intergranular glass phase seem to have formed in samples with z values 2.0 and 3.0, which is indicated by the fact that the measured z values were somewhat lower than nominal (see Table 3), and coarser β-sialon grains were formed.

Fractographic analysis shows that the β-sialons with z values of 0.6 and 1.5 (Fig. 1a and b) are intergranularly fractured, implying that the bonding between the grains is weaker than their internal strength, mainly due to the lack of any appreciable amount of intergranular glass phase. The sample with $z = 3.0$, however, has fractured transgranularly, indicating that the β-sialon grain strength decreases with increasing content of aluminium as the z value increases (see Fig. 1c).

Addition of 10 vol.% glass phase makes the β-sialon grains become more elongated (see Fig. 2a–c). Only a few elongated β-sialon grains were found with 5 vol.% glass added, but as the amount of intergranular glass phase increases, more and more β-sialon grains become elongated. It is thus to be noted that the grain morphology is strongly dependent on the amount of glass phase present for samples sintered under the same sintering conditions. A fractured surface of the sample

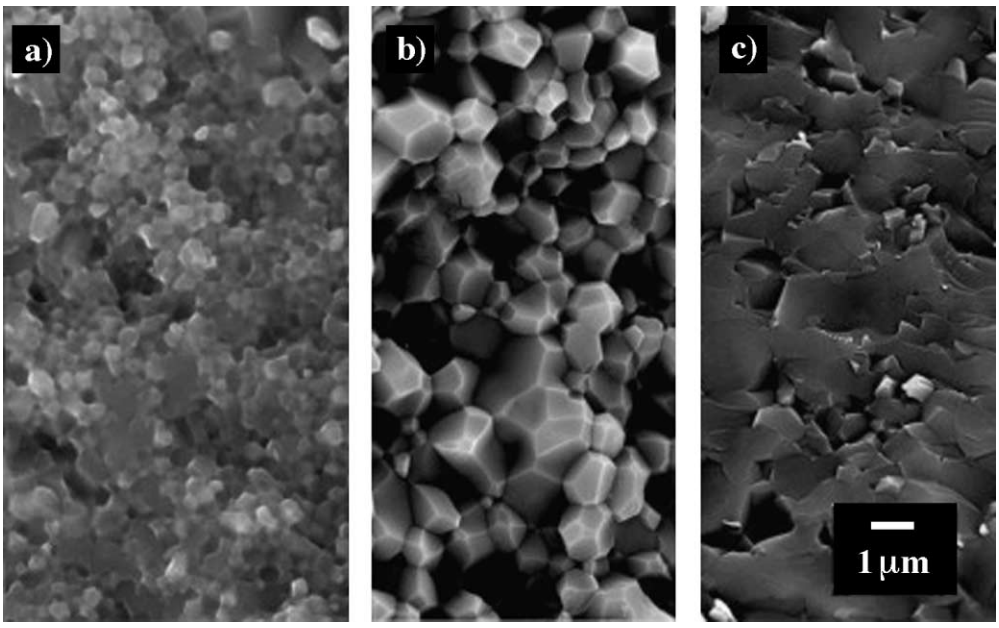

Fig. 1. Micrographs, recorded in SE mode, of fractured surfaces of the samples (a) A1, $z=0.6$; (b) A3, $z=1.5$; (c) A5, $z=3.0$. The samples did not contain any addition of extra glass.

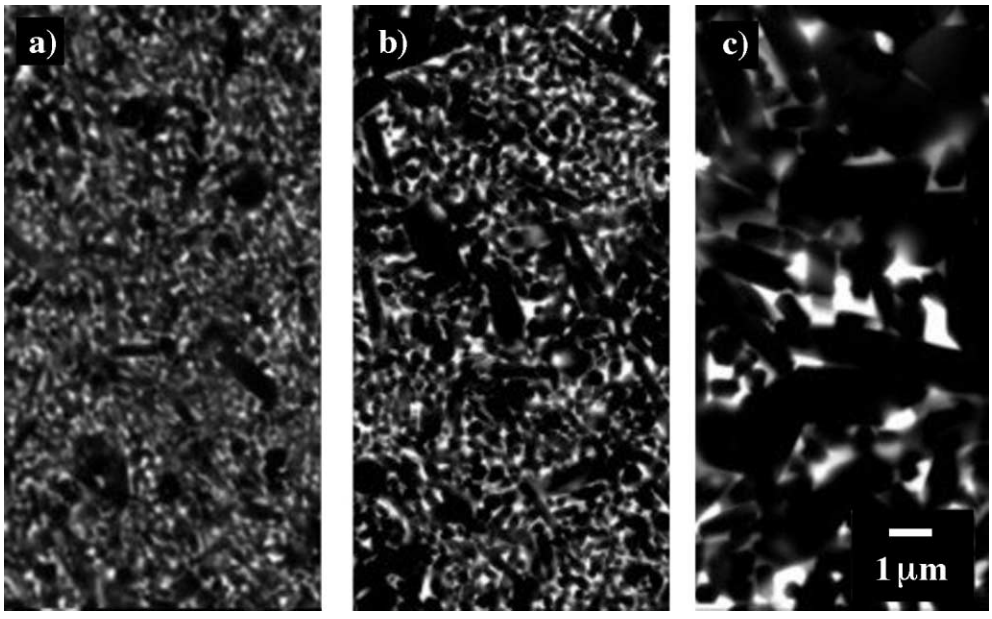

Fig. 2. Micrographs, recorded in BSE mode, of the samples (a) B2, $z=0.6$; (b) B6, $z=2.0$; (c) B8, $z=3.0$. 10 Vol.% glass is added to all three samples. The β-sialon grains are black or dark grey and the glass phase is white.

with $z=1.5$ and 10 vol.% glass (sample B5) demonstrates that the debonding and pullout effects are operative around the elongated grains, see Fig. 3. The observation indicates that these effects are responsible for the improvement of fracture toughness and thermal-shock resistance with increasing glass content (see below).

In series C, the microstructure of the β-sialon material with $z=1.5$ and 10 vol.% glass was varied by adjustment of the sintering parameters. The resulting microstructures and phase compositions are given in Fig. 4 and Table 2 respectively. The samples C1 and C2, which consist of sub-micron-sized equiaxed grains, also contain some 8% of untransformed α-Si_3N_4.

3.2. Mechanical properties

The hardness and fracture toughness values of series A samples are shown in Table 3. The z value does not influence the hardness, while the fracture toughness of

the sample with $z = 1.5$ is higher than the other compositions. The z values calculated from the unit cell parameters of the formed β-sialon phase reveal that a small amount of glass phase might have been formed in the materials, since these values are typically less than predicted, and more so for higher than for lower z values. The presence of a residual intergranular glass phase does not always imply an increase of the fracture toughness, however, because more fracture energy is consumed by debonding and/or grain boundary pull-out mechanisms. Thus, a residual intergranular glass phase combined with low-z β-sialon grains may yield an increase of fracture toughness, whereas glass combined with β-sialon grains of higher z values might not. The $z = 1.0$ sample is more fine-grained than $z = 1.5$ and, moreover, contains no glass phase, which explains its lower fracture toughness. The $z = 2.0$ sample contains somewhat more glass than $z = 1.5$, but the expected improvement in toughness was not observed, most probably because increasing aluminium content in the β-sialon grains makes them more fragile.

The hardness and fracture toughness values of series B β-sialon samples with addition of glass are also shown in Table 3. The extra glass phase has only a minor influence on the hardness of the materials. The fracture toughness improves with increasing amount of glass for low z values, but at $z = 3.0$ the presence of glass no longer has that influence. Furthermore, it is to be noted that the fracture toughness with additional glass is higher for the $z = 0.6$ samples than for those with $z = 3.0$.

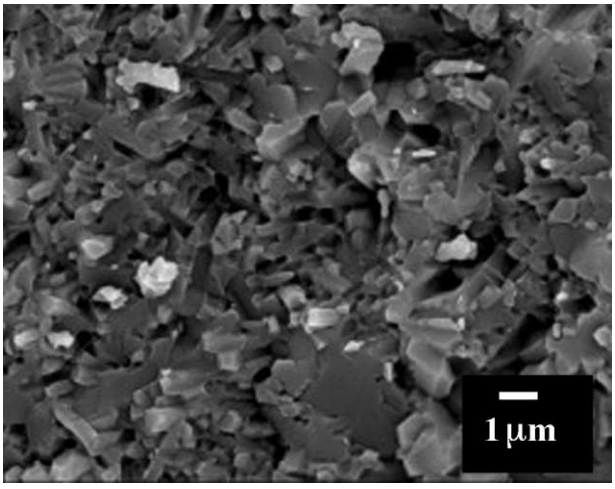

Fig. 3. Micrographs, recorded in SE mode, of a fractured surface of sample B5 with $z = 1.5$ and 10 vol.% glass. Pullout effects can be observed where elongated grains are missing.

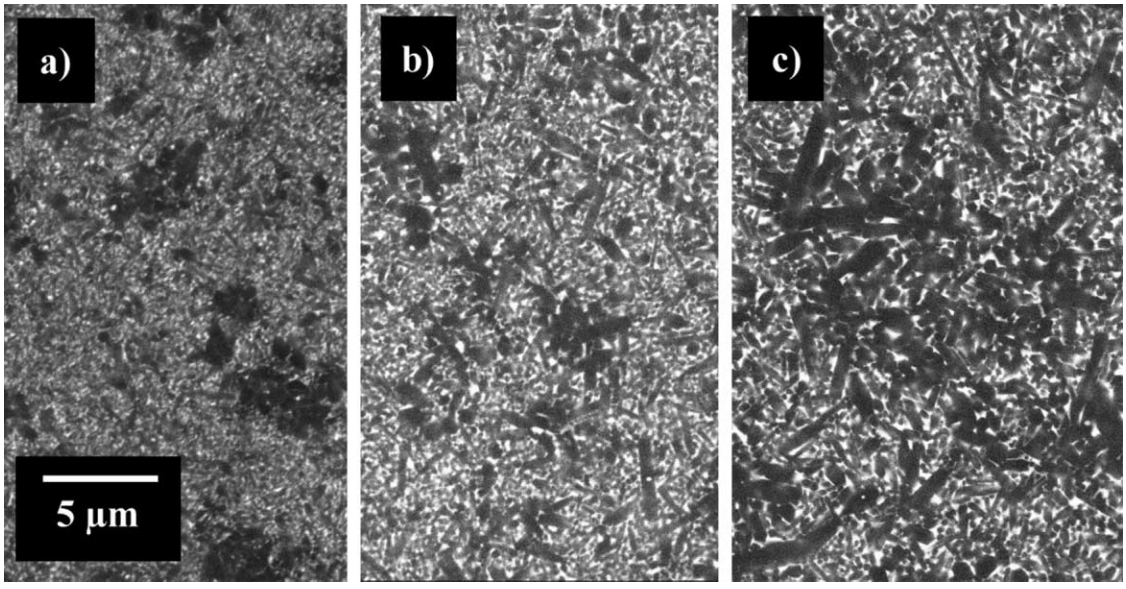

Fig. 4. Micrographs, recorded in BSE mode, of samples from series C (a) Sample C1 showing sub-micrometer-sized equiaxed grains; (b) sample C3 showing ultra-fine elongated grains; (c) sample C5 showing well developed elongated grains.

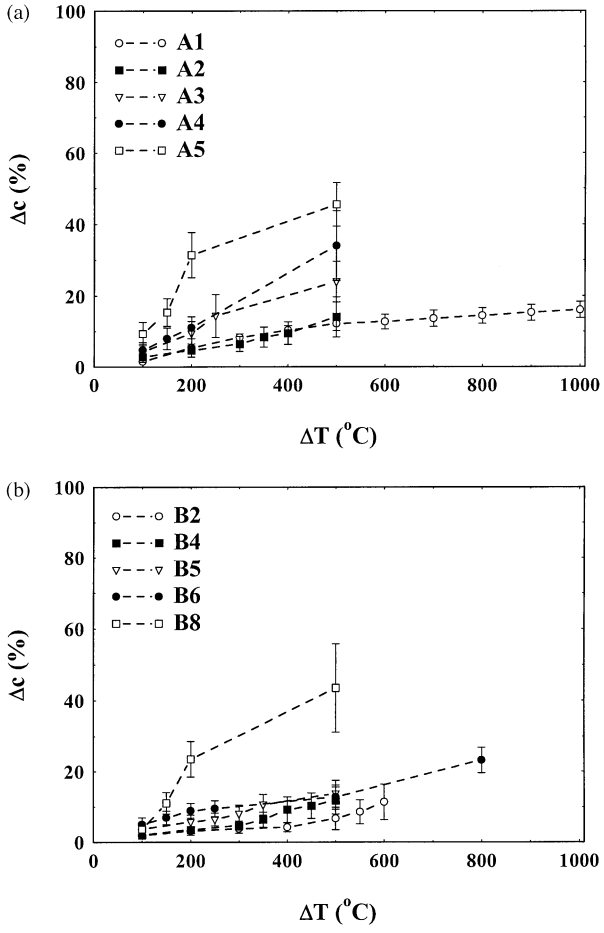

Fig. 5. Crack growth in percent plotted versus the thermal-shock temperature difference for β-sialons with different z values (a) without glass and (b) with 10% glass.

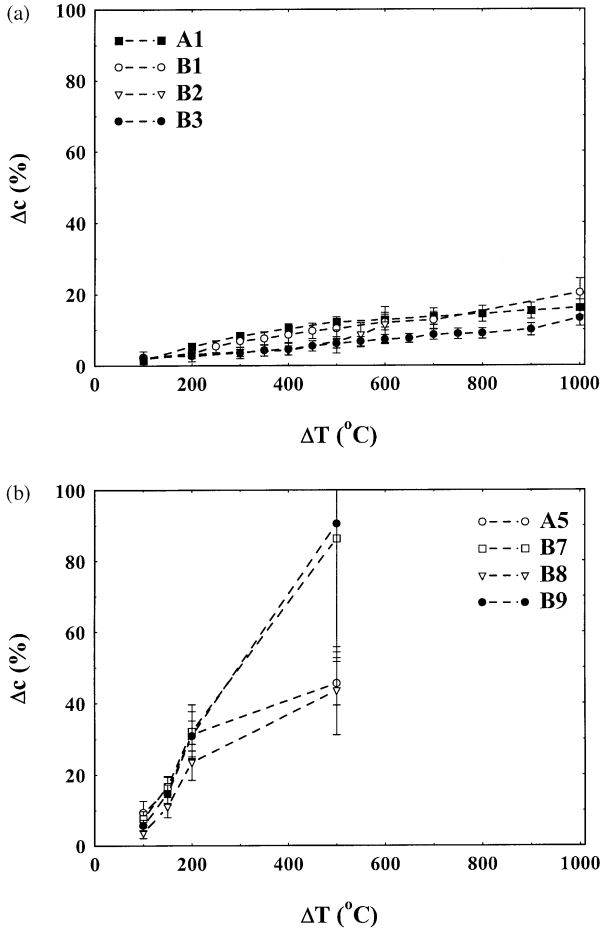

Fig. 6. Crack growth in percent plotted versus the thermal-shock temperature difference. The amount of glass is varied, keeping the z value at (a) $z=0.6$ and (b) $z=3.0$.

In series C, the fracture toughness is markedly influenced by the microstructure, thus increasing with the formation of elongated β-sialon grains and with increasing grain size. However, as expected, varying grain morphology does not influence the hardness, see Table 3.

3.3. Thermal shock properties

The crack extension versus thermal-shock temperature difference for samples of series A is shown in Fig. 5a. It is clear that the samples with lower z values are more shock resistant than those with higher z. For samples in series B with 10 vol.% glass added, the thermal-shock resistance is improved for all z values except for $z=3.0$, see Fig. 5b. At $z=0.6$, the addition of glass improves the thermal-shock resistance, and a nominal addition of 20 vol.% glass (26 vol.% measured) gave the best resistance measured in this study (see Fig. 6a). At highest z values, e.g. for $z=3.0$, the addition of glass did not improve the thermal-shock properties, see Fig. 6b.

The thermal-shock temperature difference inducing 10% crack growth (ΔT_{10}) is plotted versus the z value of the formed β-sialon in Fig. 7a–b, for samples in series A and B. Apparently the ΔT_{10} value decreases with increasing z, both with and without the presence of glass, see Fig. 7a. An increase in the amount of glass has a pronounced effect on ΔT_{10} values for low z values ($z=0.6$) but not for high values ($z=3.0$), as can be seen in Fig. 7b. The sample exhibiting the best thermal-shock resistance is the β-sialon with a z value of 0.6 and with 20 vol.% nominal addition of glass (26 vol.% measured), yielding ΔT_{10} 840 °C. The sample with $z=3.0$ had the poorest resistance to thermal shock, $\Delta T_{10} \approx 100$ °C, whatever the glass content.

The thermal-shock resistance in series C was found to be very dependent on the microstructure, and it improved markedly when elongated grains were formed, see Fig. 8. It is thus clear that the thermal-shock resistance improves with increasing fracture toughness for the samples in series B and C, which both contain the additional glass necessary for the dissolution precipitation process and the formation of elongated grains, see Fig. 9. Series C exhibits the lowest K_{1C} values for a very fine-grained morphology, and ΔT_{10} does not improve

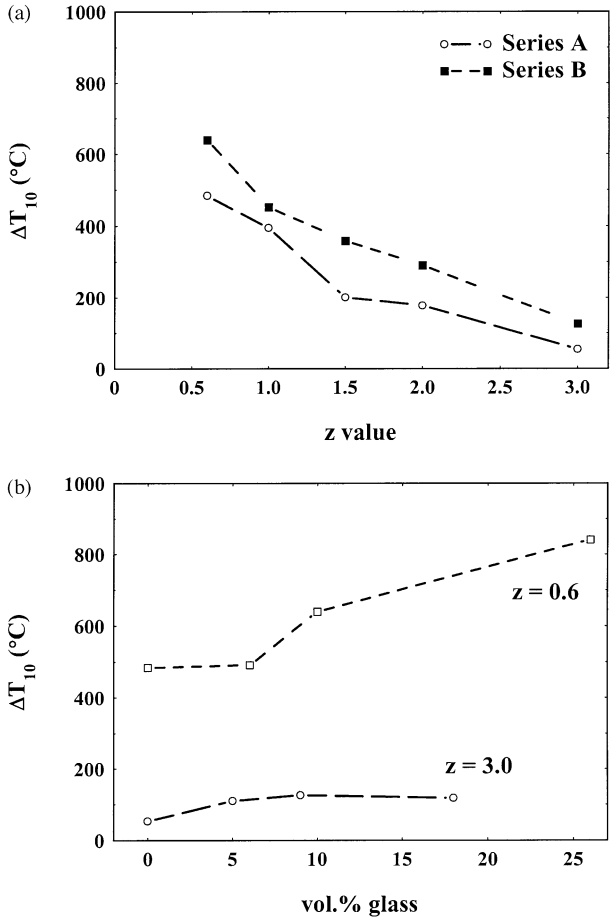

Fig. 7. The temperature difference where 10% crack growth (ΔT_{10}) occurred plotted as a function of (a) the z value and (b) the measured amount of intergranular glass phase.

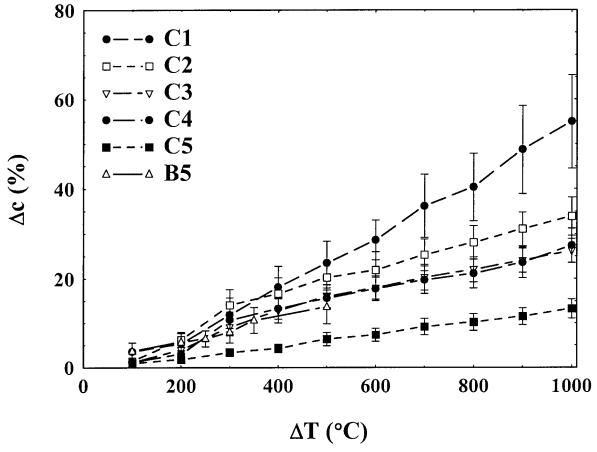

Fig. 8. Crack growth in percent plotted versus the thermal-shock temperature difference for the samples in series C and the hot-pressed sample B5, all having the composition $z = 1.5$, 10 vol.% glass. The thermal-shock resistance improves when the samples are in situ reinforced by formation of elongated grains.

until the grains become so elongated and coarse that an in situ reinforcement mechanism becomes active. When the grains are sufficiently coarse, K_{1C} reaches a value

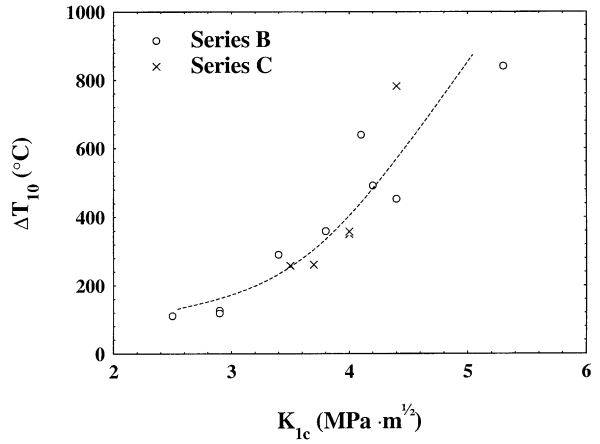

Fig. 9. The thermal-shock temperature difference inducing 10% cracks growth (ΔT_{10}) measured as a function of K_{1C} for the series B and C.

where the thermal-shock resistance improves markedly with increasing fracture toughness. From the experiments, the critical K_{1c} value seems to be around 4 MPam$^{\frac{1}{2}}$. The thermal-shock resistance of a β-sialon material is thus balanced by the z value, the amount of glass, and the morphology of the β-sialon grains.

4. Concluding remarks

An indentation-quench method, based on Vickers cracks, for measuring thermal-shock properties has been applied to β-sialon materials with different z values and amounts of yttrium-containing glass phase. The β-phase has the composition $Si_{6-z}Al_zO_zN_{8-z}$, and the z value has been varied in the range $0.6 \leqslant z \leqslant 3.0$. The method allows the use of the same sample throughout a series of increasing quenching temperature differences. The percentage crack growth is measured at each temperature step, and the statistics are improved by making several Vickers indents on the same sample.

It was found that the thermal-shock resistance is highly dependent on the z value, the amount of glass phase present, and the microstructure. The best thermal-shock resistance was found for low z values. The good thermal-shock properties of monolithic β-sialon samples with low z values can be improved even further by addition of an intergranular glass phase that is a prerequisite for formation of elongated β-grains, but for β-sialon samples with higher z values, the thermal-shock properties do not improve with addition of glass. In two series the sintering conditions were held constant and the composition was varied (z value and amount of intergranular glass). In those series the best thermal shock resistance was found for a β-sialon with a z value of 0.6, containing 20 vol.% glass. The poorest resistance was found for a sample with $z = 3.0$, and for this z value the thermal-shock properties were not improved by addition of extra glass phase. In the third series the sin-

tering conditions were varied while the composition were held constant ($z = 1.5$, 10 vol.% glass), which resulted in a series of samples with different microstructures. The grain morphology was varied from submicron sized equiaxed grains to coarse elongated grains and the thermal shock resistance was found to improve considerably for the in situ reinforced samples having elongated grains to yield about the same good thermal shock resistance as the best sample described above ($z = 0.6$, 20 vol.% glass). Thus for a β-sialon with a low z value it is possible to optimise the thermal shock resistance by balancing the z-value, the amount of intergranular glass phase, and the sintering conditions.

It is clear that microstructures containing elongated β-sialon grains improved also the fracture toughness values. These findings suggest that there is a correlation between the thermal-shock behaviour of a material and its fracture toughness value. β-sialon materials with fracture toughness $K_{1C} > 4$ MPa $m^{\frac{1}{2}}$ are those that can be most confidently expected to have good thermal-shock resistance.

Acknowledgements

This work has been performed within the Inorganic Interfacial Engineering Centre, supported by the Swedish National Board for Industrial and Technical Development (NUTEK) and by the following industrial partners: Erasteel Kloster AB, Ericsson Cables AB, Höganäs AB, Kanthal AB, OFCON Optical Fiber Consultants AB, Sandvik AB, Seco Tools AB and Uniroc AB.

References

1. Ekström, T. and Nygren, M., Sialon ceramics. *J. Am. Ceram. Soc.*, 1992, **75** (2), 259–276.
2. Buessem, W. R., Thermal shock testing. *J. Am. Ceram. Soc.*, 1955, **38**, 15–17.
3. Kingery, W. D., Factors affecting thermal stress resistance of ceramic materials. *J. Am. Ceram. Soc.*, 1955, **38**, 3–15.
4. Davidge, R. W. and Tappin, G., Thermal shock and fracture in ceramics. *Trans. Br. Ceram. Soc.*, 1967, **66**, 405–422.
5. Hasselman, D. P. H., Strength behavior of polycristalline alumina subjected to thermal shock. *J. Am. Ceram. Soc.*, 1970, **53**, 490–494.
6. Andersson, T. and Rowcliffe, D. J., Indentation thermal shock test for ceramics. *J. Am. Ceram. Soc.*, 1996, **79**, 1509–1514.
7. Pettersson, P., Johnsson, M., and Shen, Z., Evaluation of experimental parameters for measuring thermal shock properties of ceramic materials with an indentation quench method. *J. Eur. Ceram. Soc.*, in press.
8. Ekström, T., Käll, P. O., Nygren, M. and Olsson, P. O., Dense single phase β-sialon ceramics by glass encapsulated hot isostatic pressing. *J. Mat. Sci.*, 1989, **24**, 1853–1861.
9. Anstis, G. R., Chantikul, P., Lawn, B. R. and Marshall, D. B., A critical evaluation of indentation techniques for measuring fracture toughness: I Direct crack measurements.. *J. Am. Cer. Soc.*, 1981, **64**, 533–538.
10. Johansson, K. E., Palm, T. and Werner, P. E., An automatic microdensiometer for x-ray diffraction photographs. *J. Phys. E. Sci. Instrum.*, 1980, **13**, 1289–1291.
11. Werner, P. E., A Fortran program for least-squares refinement of crystal structure cell dimensions. *Arkiv för kemi*, 1969, **31**, 513–516.
12. Ramesh, R., Pomeroy, M. J., Chu, H. and Datta, P. K., Effect of gaseous environment on the corrosion of β-sialon materials. *J. Eur. Ceram. Soc.*, 1995, **15**, 1007–1014.
13. Hwang, C. M. and Tien, T.-Y., Microstructural development in silicon nitride ceramics. *Mater. Sci. Forum*, 1989, **47**, 84–109.